Tokyo Climate Center, Japan Meteorological Agency

TCC News

Spring 2020

Table of Contents: TCC News No. 60

Upgrade of the Global Ensemble Prediction System for One-month Prediction

1. Improvement of One-month Prediction

The Japan Meteorological Agency (JMA) upgraded its Global Ensemble Prediction System (Global EPS) for one-month prediction on 24th March 2020 (Yamaguchi et al. 2020). In addition to improved physical parameterization schemes in the forecast model (a low-resolution version of the Global Spectral Model (GSM)), a two-tiered Sea Surface Temperature (SST) method (Takakura and Komori, 2020) was also implemented. In this approach, the oceanic lower-boundary condition in Global EPS forecasts with lead times exceeding 11 days is relaxed from the anomaly-fixed SST to the ensemble-mean SST based on prediction using the Seasonal Ensemble Prediction System (Seasonal EPS), which is JMA's atmosphere-ocean-coupled model operationally applied for forecasts with lead times of over a month. This approach involves a much smaller computational cost than the operation of a full atmosphere-ocean coupled EPS.

The results of a 30-year hindcast experiment indicate that the forecast skill of the new Global EPS for 200-hPa velocity potential in the tropics (an important factor in predicting sub-seasonal oscillation phenomena such as the Madden-Julian Oscillation) is better than that of the previous Global EPS (Fig. 1-1). Forecast skill for four-week precipitation over many regions of Asia and the Pacific in boreal summer is also superior (Fig. 1-2).

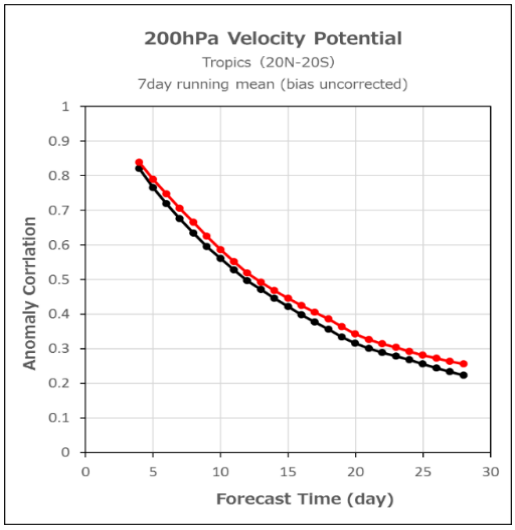

Figure 1-1 Annual average forecast skill for 200-hPa velocity potential as estimated from the 30-year hindcast experiment (1981 – 2010)
Red: anomaly correlation with the new version; black: with the previous version

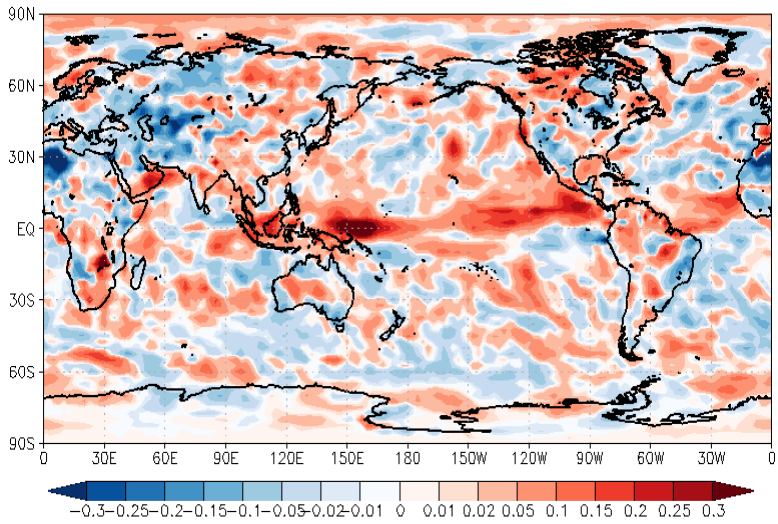

Figure 1-2 Anomaly correlation difference for four-week precipitation in boreal summer (June – August) as estimated from a 30-year hindcast experiment (1981 – 2010)
Warm and cold colors indicate improved and degraded regions respectively.

2. Release of Higher-resolution Global Gridded Data for One-month Prediction

Along with the Global EPS upgrade, JMA released higher-resolution global 1.25-degree grid data for one-month prediction in GRIB2 format, which involves spatial differencing and complex packing for reduced data volume. JMA plans to continue provision of the current low-resolution 2.5-degree grid data during the transition period over the next year or so. The data are provided to authenticated users in the following website.
https://ds.data.jma.go.jp/tcc/tcc/gpv/index.html

3. Change of Specifications in Hindcast Data for One-month Prediction

The number of hindcast ensemble members for one-month prediction was increased from 5 to 13 per initial time, and the number of initial times was reduced from 3 to 2 per month. The increase supports evaluation of model performance with smaller sampling errors and reliable probabilistic information. The hindcast data are provided to authenticated users in the same website as the previous paragraph.

4. Plans for One-month Prediction

JMA plans to upgrade its Forecast Products in Support of Early Warnings for Extreme Weather Events to a higher-resolution version within the next year, as well as to increase the horizontal and vertical resolutions of the Global EPS and improve the 2-tier SST method with upgrading of the Seasonal EPS in the near future.

5. References

Yamaguchi, H., M. Ikegami, K. Ochi, Y. Ota, R. Sekiguchi and T. Takakura, 2020: Upgrade of JMA's Global Ensemble Prediction System. CAS/JSC WGNE Res. Activ. Atmos. Oceanic Modell., submitted.

Takakura, T., and T. Komori, 2020: Two-tiered sea surface temperature approach implemented to JMA's Global Ensemble Prediction System. CAS/JSC WGNE Res. Activ. Atmos. Oceanic Modell., submitted.

(YAMADA Takashi and KOMORI Takuya)

<<Table of contents <Top of this article

Release of Global Gridded Datasets for 6-month Forecasts

JMA received requests from National Meteorological and Hydrological Services (NMHSs) and other international centers to provide forecast products with a range of six months and to accelerate the release date of long-range forecast products. In response, on 16th April 2020, JMA began providing global 2.5-degree gridded datasets for 6-month forecasts every 5-days with the following content:

- Individual forecasts of 13 ensemble members from the latest initial time
- Ensemble means and spreads based on the latest 51 forecast members using the lagged forecast method

JMA plans to continue providing these datasets for 3-month and warm/cold season predictions over a transition period spanning the next year or so. The data are provided to authenticated users at https://ds.data.jma.go.jp/tcc/tcc/gpv/index.html.

The horizontal resolution of gridded datasets remains unchanged at this time, but JMA plans to enhance this specification along with upgrading of the Seasonal Ensemble Prediction System (Seasonal EPS) in the near future.

(YAMADA Takashi)

<<Table of contents <Top of this article

El Niño Outlook (June - December 2020)

ENSO-neutral conditions persisted in May, and ENSO-neutral conditions are likely (60%) to continue until boreal autumn. (Article based on the El Niño outlook issued on 10 June 2020.)

1. El Niño/La Niña

The NINO .3 SST deviation was-0.3°C in May. SSTs in the equatorial Pacific were above normal in the western part and below normal in the eastern part (Figures 3-1 and 3-3 (a)), and subsurface temperatures were below normal from the central to eastern part (Figures 3-2 and 3-3 (b)). Atmospheric convective activity near the dateline over the equatorial Pacific was below normal, and easterly winds in the lower troposphere (i.e., trade winds) over the central equatorial Pacific were stronger than normal. These oceanic and atmospheric conditions indicate that ENSO-neutral conditions persisted in May, although some of the features of La Niña events were also present.

The subsurface cold waters, observed from the central to eastern equatorial Pacific in May, are expected to migrate eastward and to strengthen colder-than-normal SST conditions in the eastern part temporarily. JMA's El Niño prediction model suggests that the NINO.3 SST will be below normal in boreal summer temporarily, and gradually come closer to normal during boreal autumn (Figure 3-4). Based on this prediction and the observations detailed above, there is a probability of over 60% that the five-month running mean NINO.3 SST will be between-0.4 and +0.4°C in boreal summer and beyond (Figure 3-5). In conclusion, ENSO-neutral conditions are likely (60%) to continue until boreal autumn.

2. Western Pacific and Indian Ocean

The area-averaged SST in the tropical western Pacific (NINO.WEST) region was near normal in May. Values are likely to be near or above normal until boreal autumn. The area-averaged SST in the tropical Indian Ocean (IOBW) region was above normal in May. Values are likely to be above or near normal until boreal summer and near or below normal in boreal autumn.

(UMEDA Takafumi, Tokyo Climate Center)

* The SST normal for the NINO.3 region (5°S – 5°N, 150°W – 90°W) is defined as a monthly average over the latest sliding 30-year period (1990-2019 for this year).

* The SST normals for the NINO.WEST region (Eq. – 15°N, 130°E – 150°E) and the IOBW region (20°S – 20°N, 40°E – 100°E) are defined as linear extrapolations with respect to the latest sliding 30-year period, in order to remove the effects of significant long-term warming trends observed in these regions.

(a) (b)

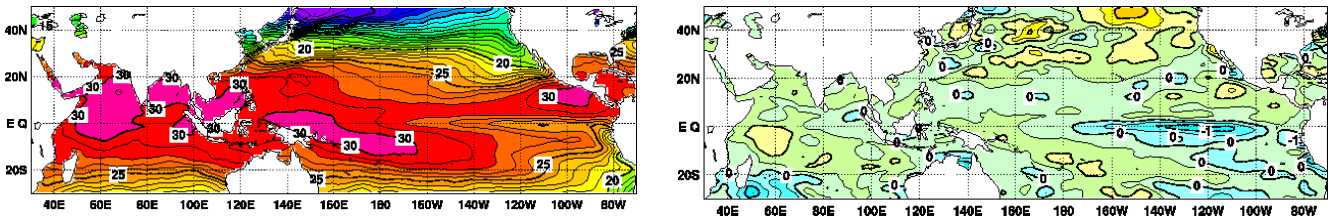

Figure 3-1 Monthly mean (a) sea surface temperatures (SSTs) and (b) SST anomalies in the Indian and Pacific Ocean areas for May 2020

The contour intervals are 1℃ in (a) and 0.5℃ in (b). The base period for the normal is 1981 – 2010.

(a) (b)

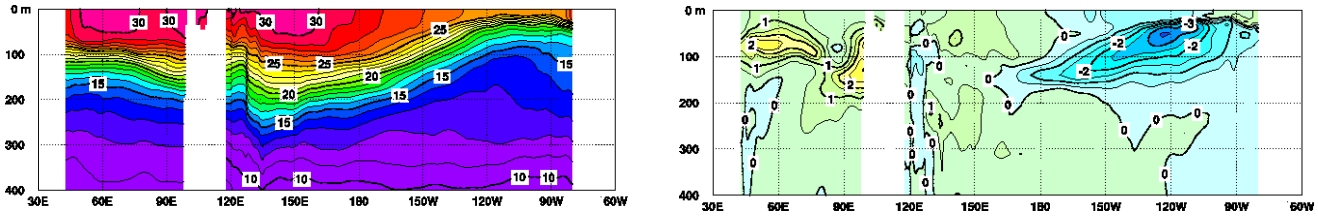

Figure 3-2 Monthly mean depth-longitude cross sections of (a) temperatures and (b) temperature anomalies in the equatorial Indian and Pacific Ocean areas for May 2020

The contour intervals are 1℃ in (a) and 0.5℃ in (b). The base period for the normal is 1981 – 2010.

(a) (b)

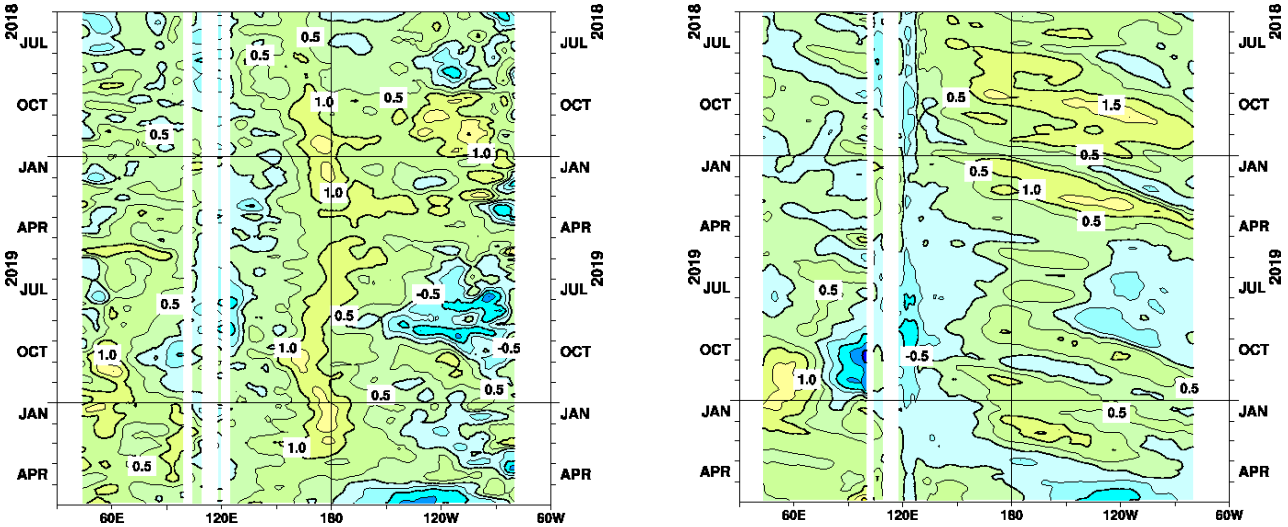

Figure 3-3 Time-longitude cross sections of (a) SST and (b) ocean heat content (OHC) anomalies along the equator in the Indian and Pacific Ocean areas

OHCs are defined here as vertically averaged temperatures in the top 300 m. The base period for the normal is 1981 – 2010.

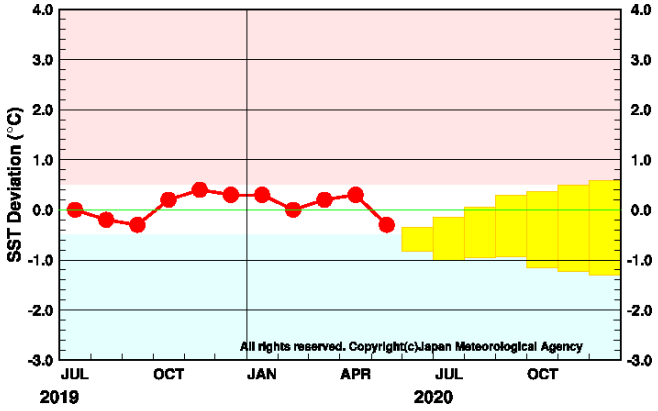

Figure 3-4 Outlook of NINO.3 SST deviation produced by the El Niño prediction model

This figure shows a time series of monthly NINO.3 SST deviations. The thick line with closed circles shows observed SST deviations, and the boxes show the values produced for up to six months ahead by the El Niño prediction model. Each box denotes the range into which the SST deviation is expected to fall with a probability of 70%.

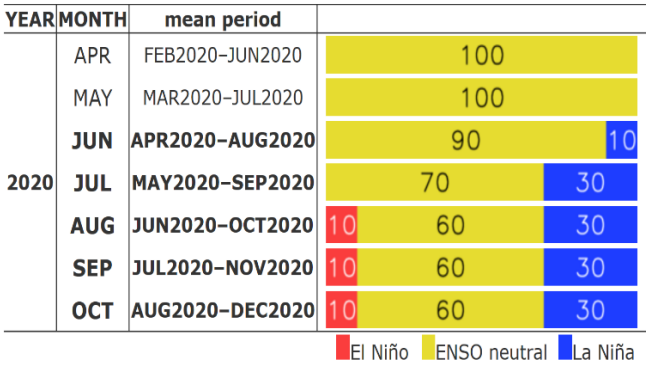

Figure 3-5 ENSO forecast probabilities based on the El Niño prediction model

Red, yellow and blue bars indicate probabilities that the five-month running mean of the NINO.3 SST deviation from the latest sliding 30-year mean will be +0.5°C or above (El Niño), between +0.4 and -0.4°C (ENSO-neutral) and -0.5°C or below (La Niña), respectively. Regular text indicates past months, and bold text indicates current and future months.

<<Table of contents <Top of this article

JMA's Seasonal Numerical Ensemble Prediction for Boreal Summer 2020

This report outlines JMA's dynamical seasonal ensemble prediction for boreal summer 2020 (June – August, referred to as JJA), which was used as a basis for JMA's operational warm-season outlook issued on 25 May 2020. The outlook is based on the seasonal ensemble prediction system of the Coupled Atmosphere-ocean General Circulation Model (CGCM).

Summary: Based on JMA's seasonal ensemble prediction system, sea surface temperature (SST) anomalies are expected to be near normal in the equatorial Pacific during boreal summer 2020, suggesting ENSO-neutral conditions. In association with above-normal SSTs in the Indian Ocean, active convection is expected over the western Indian Ocean, while inactive convection is expected over the western Pacific. Focusing on Asia, precipitation amounts are expected to be above normal from the equatorial Indian Ocean to the southern part of Southeast Asia.

1. SST anomalies (Figure4-1)

Figure 4-1 shows predicted SSTs (contours) and related anomalies (shading) for JJA. Near- or below-normal anomalies are expected in the central-to-eastern equatorial Pacific. Considering that subsurface ocean temperature anomalies in the equatorial Pacific are expected to be small (not shown), ENSO-neutral conditions are likely to continue during the period. Near- or above-normal SST anomalies are expected in the equatorial Indian Ocean, suggesting that clear IOD-like conditions may not be expected.

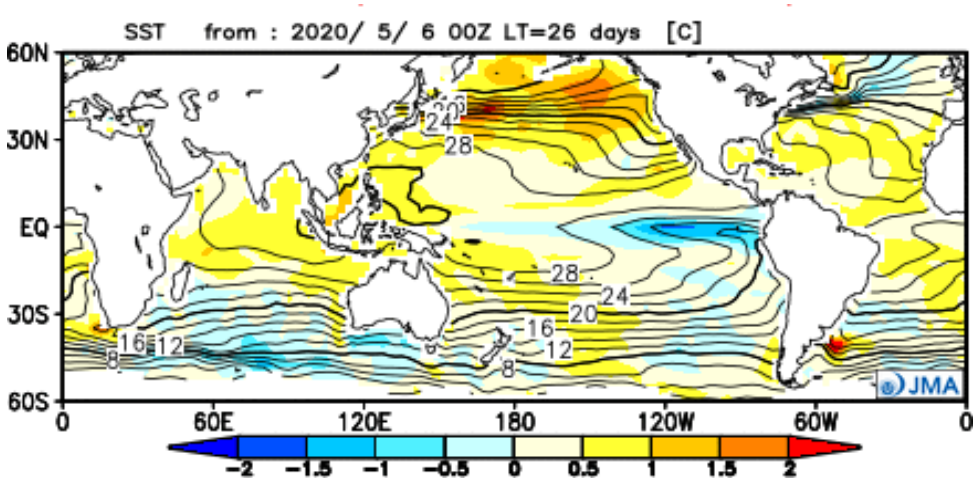

Figure 4-1 Predicted SSTs (contours) and SST anomalies (shading) for June–August 2020 (ensemble mean of 51 members)

2. Prediction for the tropics and sub-tropics (Figure4-2)

Figure 4-2 (a) shows predicted precipitation (contours) and related anomalies (shading) for JJA. In association with above-normal SSTs in the Indian Ocean, above-normal anomalies are expected in and around the southern part of South Asia and from the equatorial Indian Ocean to the southern part of Southeast Asia. Below-normal anomalies are expected in the seas east of the Philippines and around the date line in the equatorial Pacific.

Figure 4-2 (b) shows predicted velocity potential (contours) and related anomalies (shading) in the upper troposphere (200 hPa) for JJA. In association with the predicted SST and precipitation anomalies discussed above, negative (i.e., divergent) anomalies are expected over the western Indian Ocean, while positive (i.e., convergent) anomalies are expected around the date line in the equatorial Pacific.

Figure 4-2 (c) shows predicted stream functions (contours) and related anomalies (shading) in the upper troposphere (200 hPa) for JJA. Negative (i.e., cyclonic) anomalies are expected over the seas east of the Philippines, indicating that the southeastward extension of the Tibetan High may be weaker than normal.

Figure 4-2 (d) shows predicted stream functions (contours) and related anomalies (shading) in the lower troposphere (850 hPa) for JJA. In association with active convection over the Indian Ocean, equatorial symmetric cyclonic anomalies are expected in the Indian Ocean, reflecting an active Indian Monsoon. Equatorial symmetric anti-cyclonic anomalies are expected over the western-to-central Pacific in association with inactive convection over the Pacific.

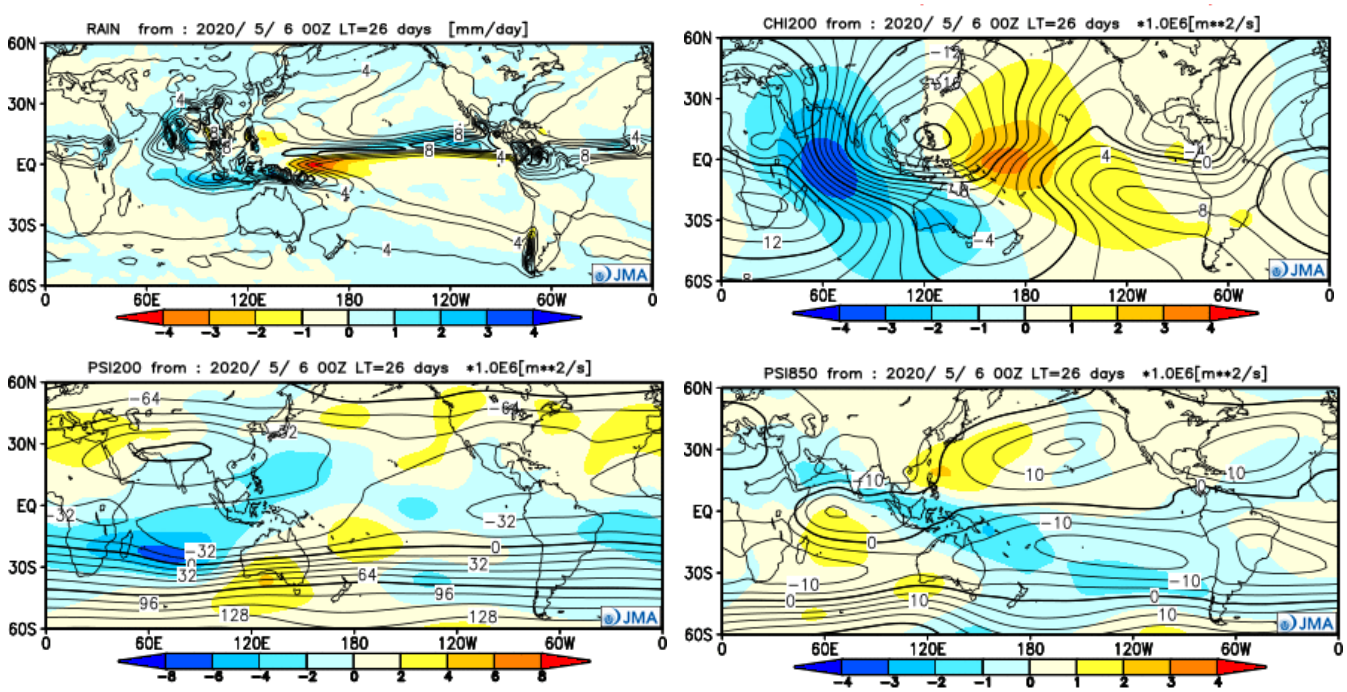

Figure 4-2 Predicted atmospheric fields from 60°N –60°S for June–August 2020 (ensemble mean of 51 members)
(a) Precipitation (contours) and anomaly (shading). The contour interval is 2 mm/day. (b) Velocity potential at 200 hPa (contours) and anomaly (shading). The contour interval is 2×10^6 m^2/s. (c) Stream function at 200 hPa (contours) and anomaly (shading). The contour interval is 16×10^6 m^2/s. (d) Stream function at 850 hPa (contours) and anomaly (shading). The contour interval is 5×10^6 m^2/s.

3. Prediction for the mid- and high- latitudes of the Northern Hemisphere (Figure4-3)

Figure 4-3 (a) shows predicted geopotential heights (contours) and related anomalies (shading) at 500 hPa for JJA. Positive anomalies are expected over most of the Northern Hemisphere in association with global warming trends.

Figure 4-3 (b) shows predicted sea level pressure (contours) and related anomalies (shading) for JJA. In association

with relatively small anomalies in geopotential height at 500 hPa, negative anomalies are expected over the northern polar region, eastern China and the eastern part of the North Pacific.

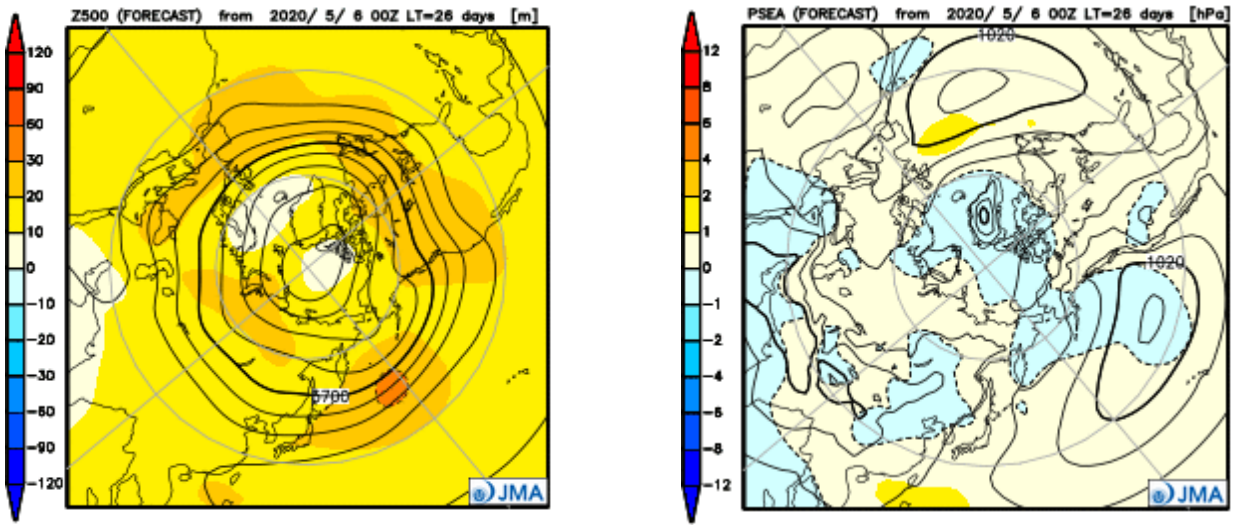

Figure 4-3 Predicted atmospheric fields from 20°N–90°N for June–August 2020 (ensemble mean of 51 members)
(a) Geopotential height at 500 hPa (contours) and anomaly (shading). The contour interval is 60 m. (b) Sea level pressure (contours) and anomaly (shading). The contour interval is 4 hPa.

Note: JMA operates a seasonal Ensemble Prediction System (EPS) using the Coupled atmosphere-ocean General Circulation Model (CGCM) to make seasonal predictions beyond a one-month time range. The EPS produces perturbed initial conditions by means of a combination of the initial perturbation method and the lagged average forecasting (LAF) method. The prediction is made using 51 members from the latest four initial dates (13 members are run every 5 days). Details of the prediction system and verification maps based on 30-year hindcast experiments (1981–2010) are available at http://ds.data.jma.go.jp/tcc/tcc/products/model/.

(ISHIZAKI Shiro, Tokyo Climate Center)

<<Table of contents <Top of this article

Summary of the 2019/2020 Asian Winter Monsoon

This report summarizes the characteristics of the surface climate and atmospheric/oceanographic considerations related to the Asian winter monsoon for 2019/2020.

Note: The Japanese 55-year Reanalysis (JRA-55; Kobayashi et al. 2015) atmospheric circulation data and COBE-SST (Ishii et al. 2005) sea surface temperature (SST) data were used for this investigation. NOAA Interpolated Outgoing Longwave Radiation (OLR) data (Liebmann and Smith 1996) provided by the U.S. NOAA Earth System Research Laboratory (ESRL) from their web site at https://www.esrl.noaa.gov/psd/ was referenced to infer tropical convective activity. The base period for the normal is 1981 to 2010. The term "anomaly" as used in this report refers to deviation from the normal.

1. Surface climate conditions

Temperatures for December 2019 to February 2020 (Figure 5-1) were above normal in many parts of Asia and Siberia, with the exception of the area from central China to the northern part of South Asia. In particular, very warm conditions continued throughout the period from eastern Japan to southeastern China and in the southern part of South Asia. Seasonal mean temperatures in Japan, Korea and Russia were the highest for winter since 1897/1898 (Japan Meteorological Agency), 1972/1973 (Korea Meteorological Administration) and 1890/1891 (Hydrometcenter of Russia), respectively.

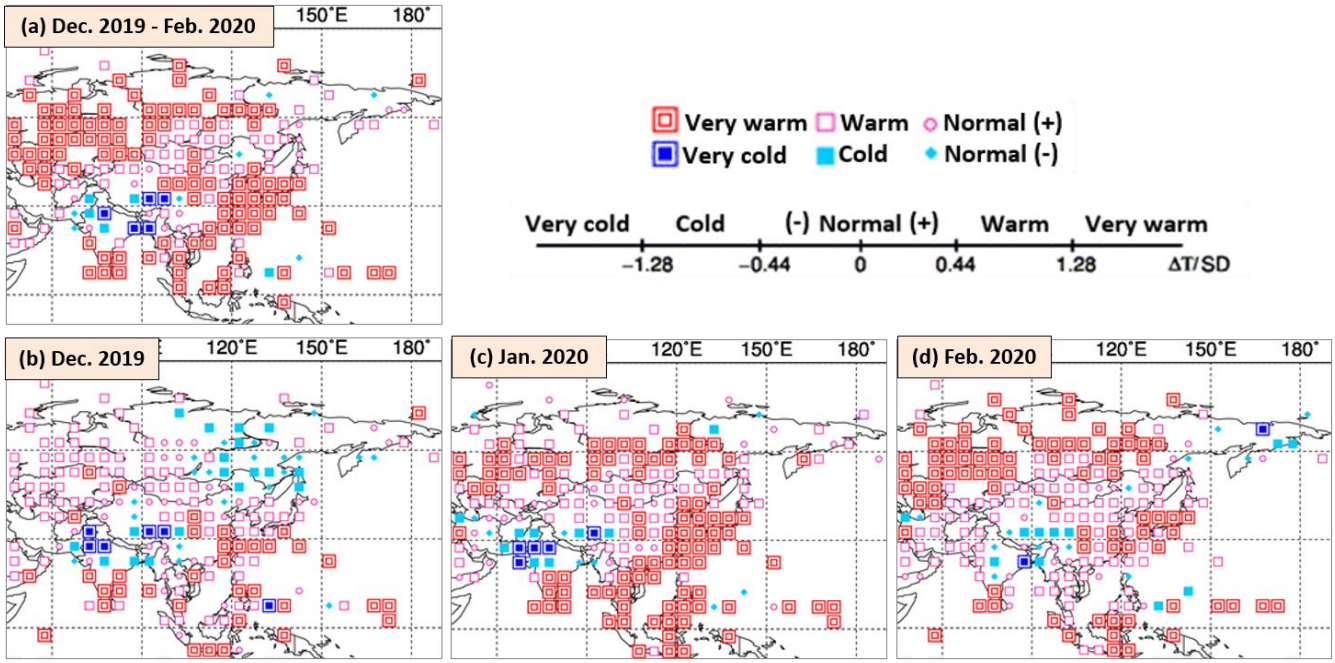

Figure 5-1 (a) Three-month mean temperature anomalies for December 2019 to February 2020, and monthly mean temperature anomalies for (b) December 2019, (c) January 2020 and (d) February 2020

Categories are defined by the three-month/monthly mean temperature anomaly against the normal divided by its standard deviation and averaged in 5° × 5° grid boxes. The thresholds of each category are -1.28, -0.44, 0, +0.44 and +1.28. Standard deviations were calculated from 1981- 2010 statistics. Areas over land without graphical marks are those where observation data are insufficient or where normal data are unavailable.

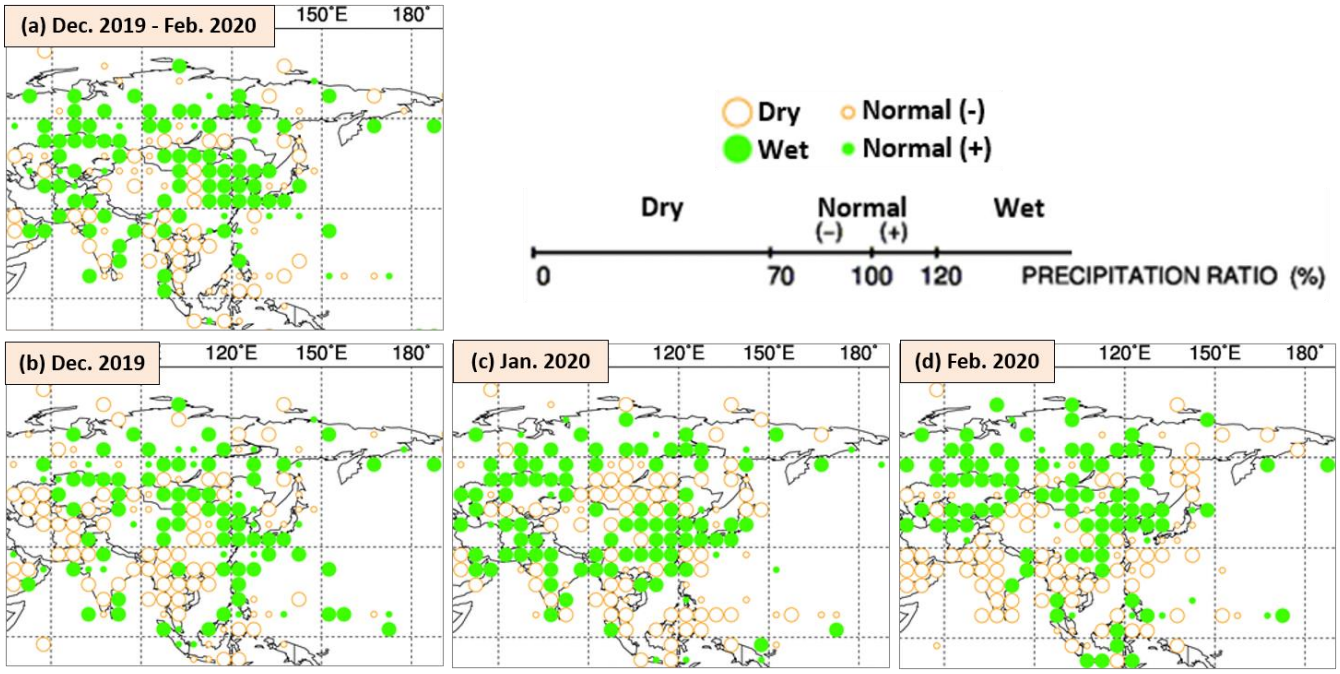

Figure 5-2 (a) Three-month precipitation ratio for December 2019 to February 2020, and monthly precipitation ratio for (b) December 2019, (c) January 2020 and (d) February 2020

Categories are defined by the three-month/monthly precipitation ratio against the normal and averaged in 5° × 5° grid boxes. The thresholds of each category are 70, 100 and 120%. Areas over land without graphical marks are those where observation data are insufficient or where normal data are unavailable.

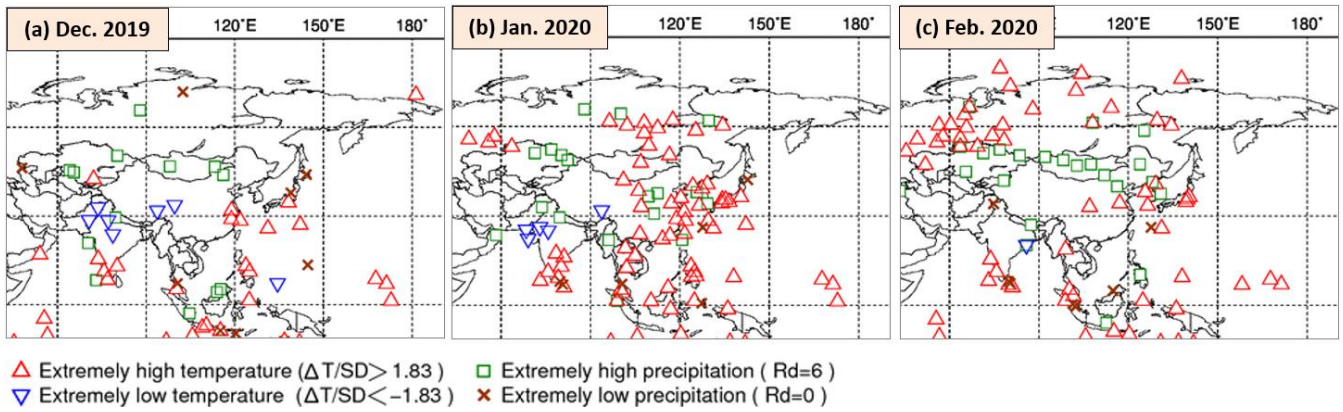

Figure 5-3 Extreme climate stations for (a) December 2019, (b) January 2020 and (c) February 2020

ΔT, SD and Rd indicate temperature anomaly, standard deviation and quintile, respectively.

Precipitation amounts during this period (Figure 5-2) were above normal in the eastern part of East Asia, from the western part of Eastern Siberia to Central Siberia, and in and around Central Asia, and were below normal in the northern part of Southeast Asia.

Figure 5-3 shows extreme climate conditions observed between December 2019 and February 2020. In December, extremely high temperatures were seen in southern India and the southern part of Southeast Asia, and extremely low temperatures were seen from northeastern Pakistan to central India. In January, extremely high temperatures

were seen in and around the central part of Central Siberia, from eastern to central East Asia, in Southeast Asia, and from southern India to Sri Lanka, while extremely low temperatures were seen from western India to southern Pakistan. Extremely high precipitation amounts were observed in northeastern Kazakhstan. In February, extremely high temperatures were seen from the northwestern part of Eastern Siberia to the northern part of Western Siberia, from the central part of Western Siberia to the northwestern part of Central Asia, from eastern Japan to central China, from southwestern India to Sri Lanka, and in the southern part of Southeast Asia. Extremely high precipitation amounts were observed from northeastern China to the central part of Central Asia.

2. Characteristic atmospheric circulation and oceanographic conditions

2.1 Conditions in the tropics

In the equatorial Pacific, remarkably positive SST anomalies were observed in the western part. In the North Pacific, remarkably positive SST anomalies were observed from east of the Philippines to far east of Japan and in central and eastern tropical regions. In the Indian Ocean, remarkably positive SST anomalies were observed across almost the entire tropical region (Figure 5-4).

Convective activity inferred from OLR during this period (Figure 5-5) was persistently enhanced over the western tropical Indian Ocean and around the date line in the equatorial Pacific, reflecting higher-than-normal SSTs in these regions, and was suppressed over the Maritime Continent.

In the upper troposphere, large-scale divergent anomalies were seen over the western Indian Ocean and around the date line in association with enhanced convective activity, and convergent anomalies were observed over the Maritime Continent (Figure 5-6 (a)). In the 200-hPa stream function field (Figure 5-6 (b)), a wave train was seen from Europe to Japan along the subtropical jet stream, with anti-cyclonic circulation anomalies over the Arabian Sea and Japan, and cyclonic circulation anomalies over southern China. This meandering of the jet stream was associated with enhanced convection over the western Indian Ocean and suppressed convection over the Maritime Continent, and partly originated from the northward meandering of the westerly jet stream over Europe. In the lower troposphere (Figure 5-6 (c)), anti-cyclonic circulation anomalies straddling the equator were seen from the central tropical Indian Ocean to the Maritime Continent in association with suppressed convection over the Maritime Continent, and cyclonic circulation anomalies straddling the equator were seen west of the date line in the tropical Pacific.

The active phase of equatorial intraseasonal oscillation propagated eastward globally during winter 2019/2020, overlapping with persistently enhanced convective activity over the western Indian Ocean and around the date line (Figure 5-7).

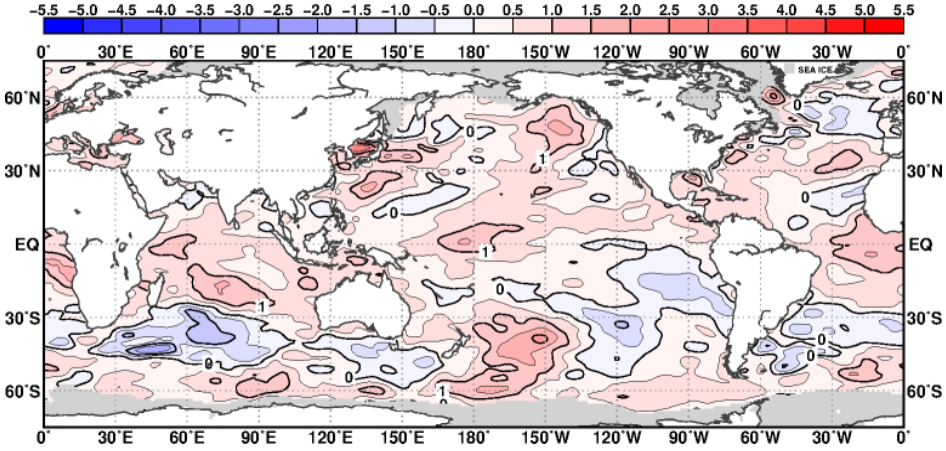

Figure 5-4 Three-month mean sea surface temperature (SST) anomalies [°C] for December 2019 to February 2020

The contour interval is 0.5°C.

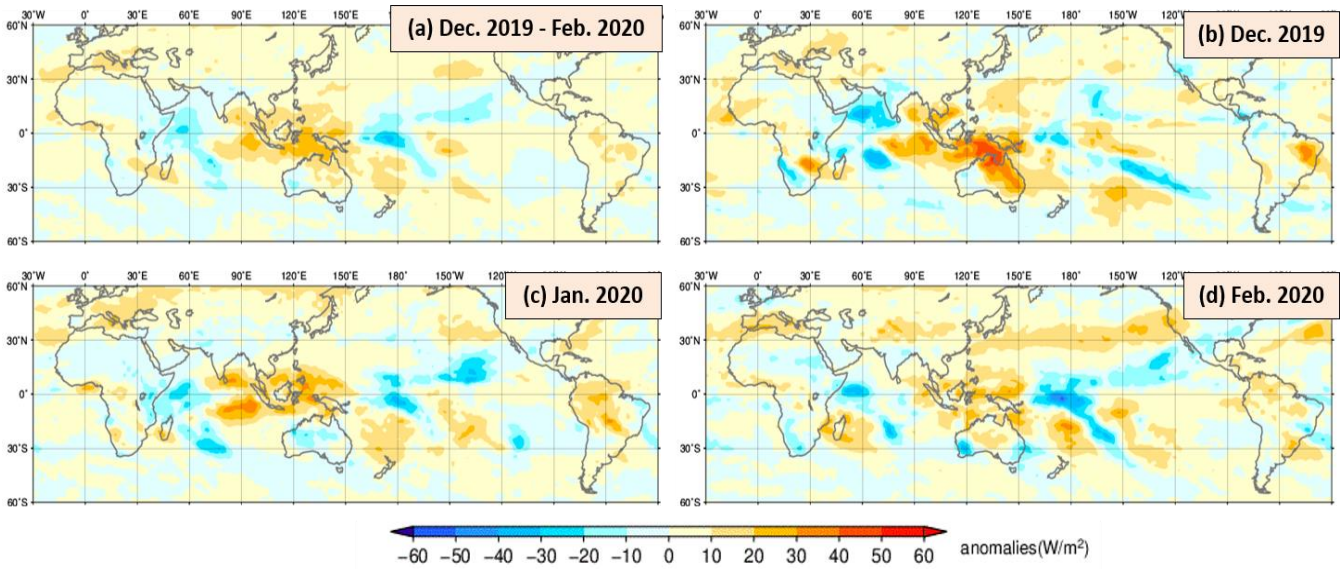

Figure 5-5 Outgoing longwave radiation (OLR) anomalies [W/m^2] for (a) December 2019 to February 2020, (b) December 2019, (c) January 2020 and (d) February 2020

The blue and red shading indicates areas of enhanced and suppressed convective activity, respectively.

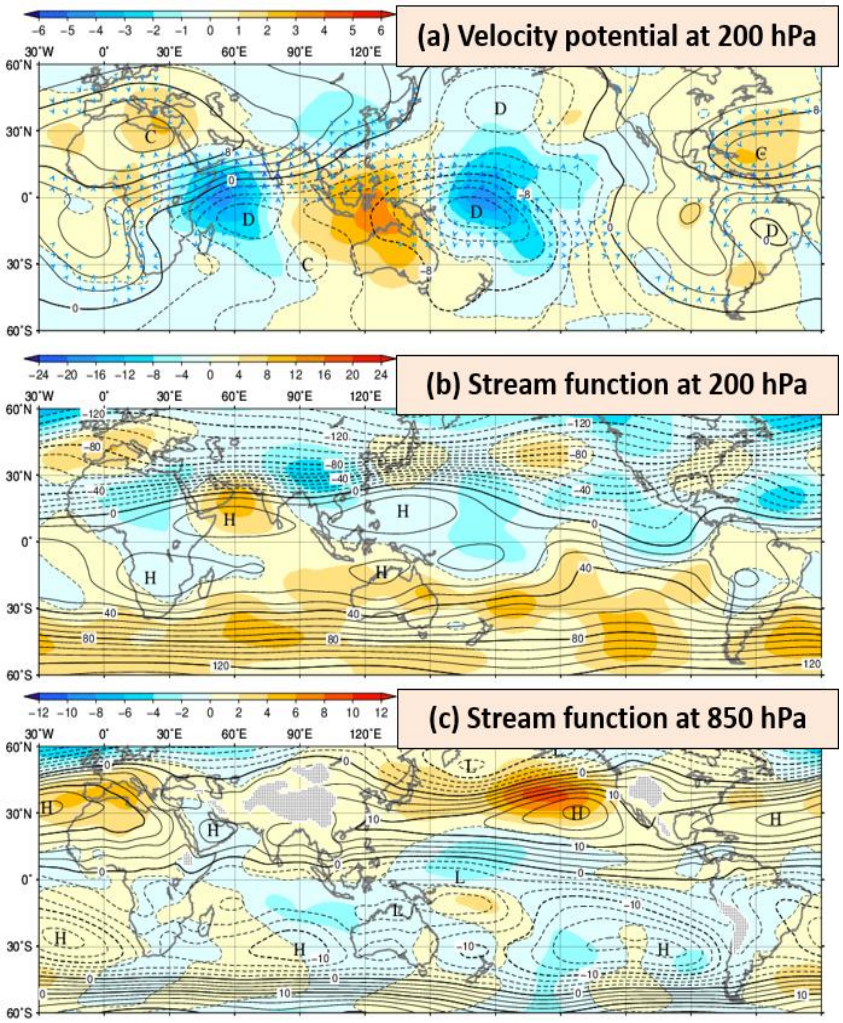

Figure 5-6 Three-month mean (a) 200-hPa velocity potential, (b) 200-hPa stream function and (c) 850-hPa stream function for December 2019 to February 2020 [unit: 10^6 m^2/s]

(a) The contours indicate velocity potential at intervals of 2 × 10^6 m^2/s, and the shading shows velocity potential anomalies. D and C indicate the bottom and the peak of velocity potential, corresponding to the centers of large-scale divergence and convergence, respectively. The vectors show divergent wind. (b, c) The contours indicate stream function at intervals of (b) 10 × 10^6 m^2/s and (c) 2.5 × 10^6 m^2/s, and the shading shows stream function anomalies. H and L denote the centers of anti-cyclonic and cyclonic circulations, respectively.

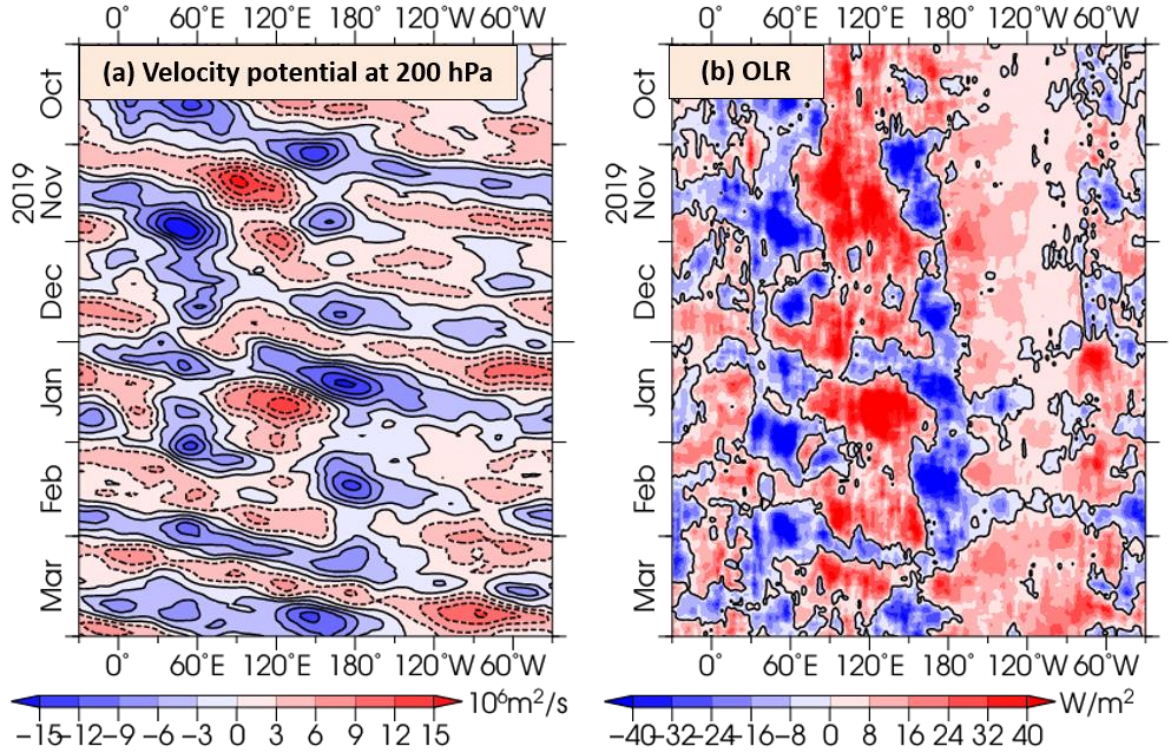

Figure 5-7 Time-longitude cross section of seven-day running mean (a) 200-hPa velocity potential anomalies [10^6 m^2/s] and (b) outgoing longwave radiation (OLR) anomalies [W/m^2] around the equator (5°S – 5°N) for October 2019 to March 2020

(a) The blue and red shading indicates areas of divergence and convergence anomalies, respectively. (b) The blue and red shading indicates areas of enhanced and suppressed convective activity, respectively.

2.2 Conditions in the extratropics

In the 500-hPa height field during winter 2019/2020 (Figure 5-8), positive anomalies were seen over Japan, the mid-latitudes in the central and eastern North Pacific, and southern Europe, while negative anomalies were seen over Alaska and near Iceland. As shown in Figure 5-9, the positive phase of the Arctic Oscillation (AO; also known as the Northern Annular Mode) with negative anomalies over the northern polar region and positive anomalies over the Northern Hemisphere mid-latitudes was dominant in January and February. The Aleutian Low and the Siberian High were weaker than normal during winter 2019/2020, indicating a weaker-than-normal East Asian Winter Monsoon that contributed to the extremely warm conditions observed in East Asia.

The polar front jet stream was clearly seen over northern Eurasia in association with the positive AO, which is linked with weak cold-air mass accumulation over a broad area from Europe to Siberia. The subtropical jet stream shifted southward of its normal position from the northern part of South Asia to southern China and meandered northward over the mid-latitudes in the western North Pacific (Figure 5-10 (a)). These conditions contributed to weaker-than-normal cold-air flow over East Asia. Temperatures at 850 hPa were above normal from Europe via Central Siberia to Japan, and below normal over the northern part of South Asia (Figure 5-10 (b)).

(SATO Hitoshi, Tokyo Climate Center)

References

Ishii, M., A. Shouji, S. Sugimoto and T. Matsumoto, 2005: Objective analyses of sea-surface temperature and marine meteorological variables for the 20th century using ICOADS and the Kobe Collection. *Int. J. Climatol.*, **25**, 865-879.

Kobayashi, S., Y. Ota, Y. Harada, A. Ebita, M. Moriya, H. Onoda, K. Onogi, H. Kamahori, C. Kobayashi, H. Endo, K. Miyaoka, and K. Takahashi, 2015: The JRA-55 Reanalysis: General specifications and basic characteristics. *J. Meteor. Soc. Japan*, **93**, 5 – 48.

Liebmann, B., and C. A. Smith, 1996: Description of a complete (interpolated) outgoing longwave radiation dataset. *Bull. Amer. Meteor. Soc.*, **77**, 1275–1277.

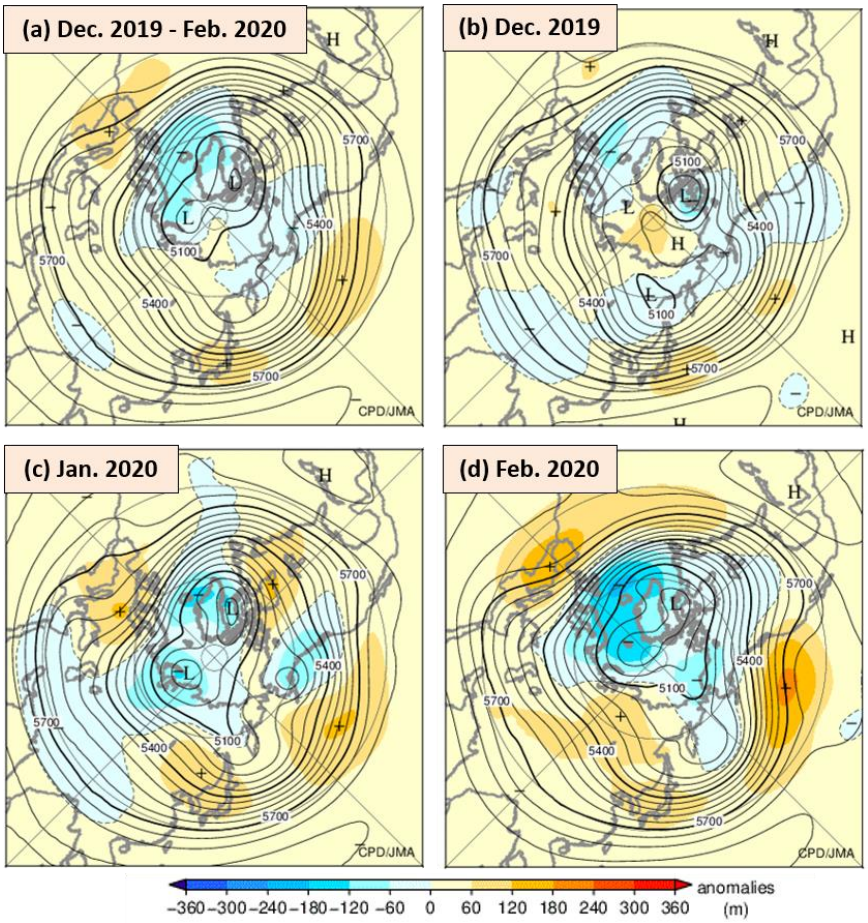

Figure 5-8 500-hPa height [m] for (a) December 2019 to February 2020, (b) December 2019, (c) January 2020 and (d) February 2020

The contours indicate height at intervals of 60 m, and the shading denotes height anomalies. H and L indicate the peak and bottom of 500-hPa height, respectively, and + (plus) and – (minus) show the peak and bottom of anomalies, respectively.

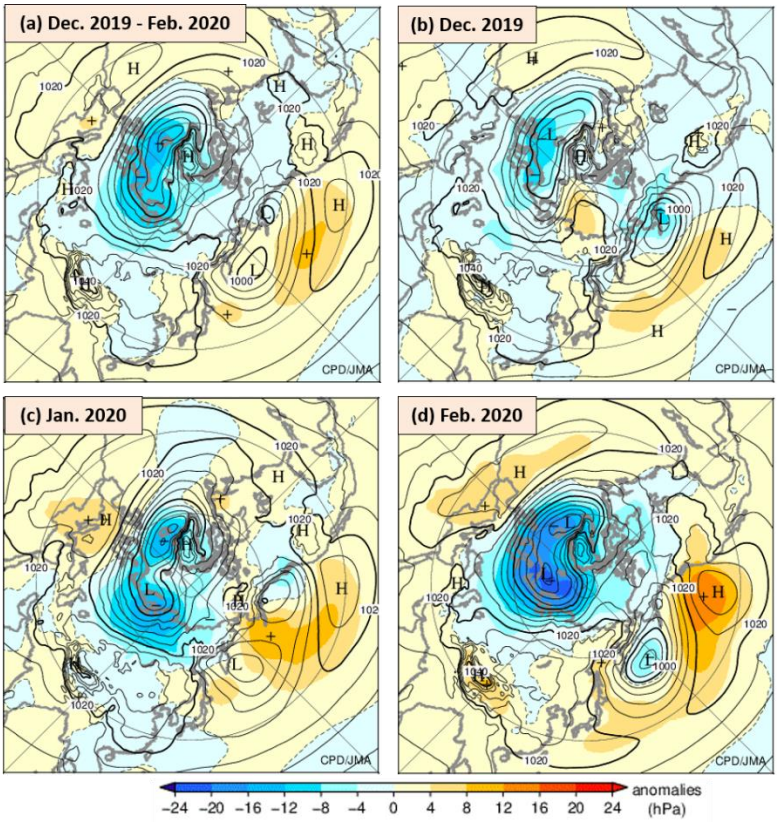

Figure 5-9 Sea level pressure [hPa] for (a) December 2019 to February 2020, (b) December 2019, (c) January 2020 and (d) February 2020

The contours indicate sea level pressure at intervals of 4 hPa, and the shading shows related anomalies. H and L indicate the centers of high and low pressure systems, respectively, and + (plus) and – (minus) show the peak and bottom of sea level pressure anomalies, respectively.

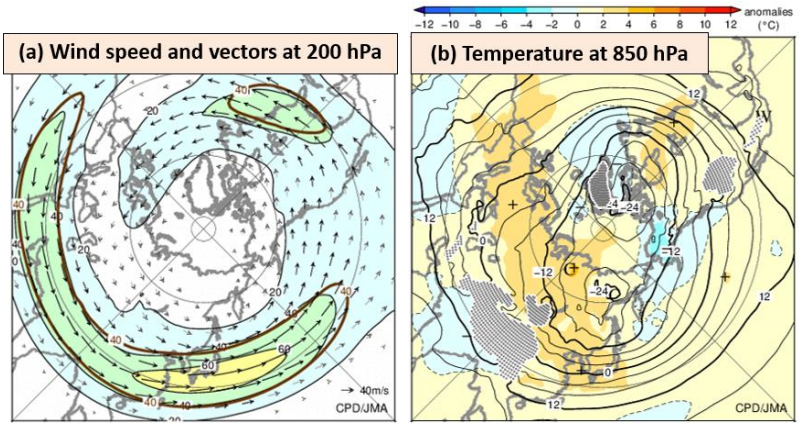

Figure 5-10 Three-month mean (a) 200-hPa wind speed and vectors [m/s] and (b) 850-hPa temperature [°C] for December 2019 to February 2020

(a) The black lines show wind speed at intervals of 20 m/s and the brown lines show its normal at intervals of 40 m/s. (b) The contours indicate temperature at intervals of 4 °C and the shading shows related anomalies.

<<Table of contents <Top of this article

Climate Characteristics of Japan's Warmest-ever Winter

TCC issued a press release regarding climate characteristics of Japan's warmest-ever winter 2019/2020. An abstract of the press release and the download link for the full article are as follows.

Winter 2019/20 (December to February) was the warmest on record for Japan, with an average temperature anomaly of 1.66°C above normal.

The Japan Meteorological Agency and its Advisory Panel on Extreme Climatic Events[1] attributed this extreme to a persistent northward meandering of the subtropical jet stream over and around Japan. The Arctic Oscillation in its positive phase also dominated atmospheric circulation over the Northern Hemisphere from January onward, resulting in a lower incidence of typical surface pressure patterns associated with the East Asian Winter Monsoon in Japan and weaker-than-normal southward cold-air flow over the country. Global warming may also have contributed to these exceptionally warm winter conditions.
URL: http://ds.data.jma.go.jp/gmd/tcc/tcc/news/press_20200501.pdf

(MOCHIZUKI Yasushi, Tokyo Climate Center)

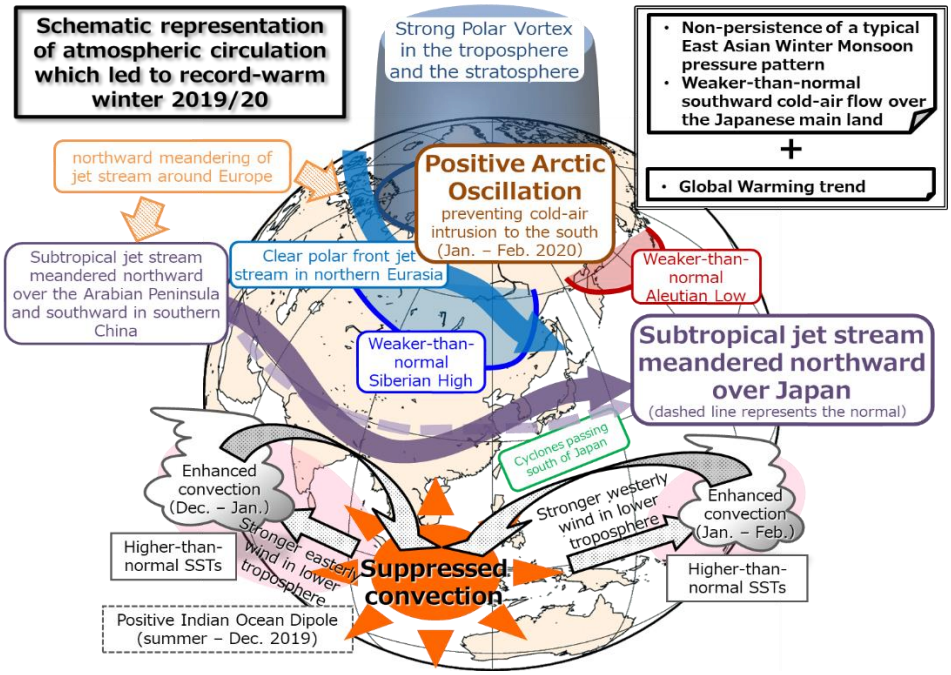

Figure 6-1 Atmospheric circulation conditions associated with the climate extremes observed in winter 2019/20

<<Table of contents <Top of this article

[1] The JMA Advisory Panel, consisting of prominent experts on climate science from universities and research institutes, was established in June 2007 by JMA to investigate extreme climate events based on up-to-date information and findings. The current chair is Prof. Hisashi Nakamura from the University of Tokyo. See TCC News No. 56 for more details on the outline and the framework of the Panel.

TCC contributions to Regional Climate Outlook Forums in Asia

WMO Regional Climate Outlook Forums (RCOFs) bring together national, regional and international climate experts on an operational basis to produce regional climate outlooks based on input from participating NMHSs, regional institutions, Regional Climate Centres (RCCs) and global producers of climate predictions. By providing a platform for countries with similar climatological characteristics to discuss related matters, these forums ensure consistency in terms of access to and interpretation of climate information.

In spring 2020, against the background of the worldwide COVID‐19 outbreak, TCC experts gave online presentations detailing the Center's climate outlook at:

- the 16th session of the Forum on Regional Climate Monitoring, Assessment and Prediction for Regional Association II (FOCRA II)
- the 16th summer session of the South Asian Climate Outlook Forum (SASCOF-16)

As part of WMO World Meteorological Centre (WMC) and RCC activities, TCC experts provided a summer monsoon season outlook based on JMA's dynamical seasonal ensemble prediction system, with probabilistic information on atmospheric circulation patterns and the evolution of conditions in the tropical Pacific and Indian Ocean areas. A WMC Tokyo expert also chaired a session on the establishment of a consensus outlook for the South Asian region. The discussion and the outcomes of these online sessions are expected to support the output of country-scale outlooks by National Meteorological and Hydrological Services (NMHSs) in the relevant regions.

(FOCRA II: OIKAWA Yoshinori,
SASCOF-16: KOMORI Takuya, Tokyo Climate Center)

<<Table of contents <Top of this article

You can also find the latest newsletter from Japan International Cooperation Agency (JICA).
JICA's World (April 2020)
https://www.jica.go.jp/english/publications/j-world/2004.html
JICA's World is the quarterly magazine published by JICA. It introduces various cooperation projects and partners along with the featured theme. The latest issue features "Nutrition for Growth: Toward Better Nutrition for All".

Any comments or inquiry on this newsletter and/or the TCC website would be much appreciated.
Please e-mail to tcc@met.kishou.go.jp.
(Editors: Oikawa Yoshinori, Mochizuki Yasushi and Tsuji Kazuaki)

Tokyo Climate Center, Japan Meteorological Agency
1-3-4 Otemachi, Chiyoda-ku, Tokyo 100-8122, Japan

TCC Website:
https://ds.data.jma.go.jp/tcc/tcc/index.html

<<Table of contents